ACTIVATION TECHNIQUE OF ASTROPHYSICAL PHOTONUCLEAR REACTION RATE MEASUREMENTS USING BREMSSTRAHLUNG

I. Semisalov**, Ye. Skakun, V. Kasilov, V. Popov

National Science Center "Kharkov Institute of Physics and Technology", 61108, Kharkov, Ukraine

(Received January 22, 2013)

Astrophysical simulation of natural abundance of p-nuclei needs knowledge of the enormous quality of photonuclear reaction rates which can be derived from the reaction integral yields. The applicability of the activation technique for getting relevant experimental information is shown by the examples of the (γ, n)-reactions running in the ^{96}Ru and ^{98}Ru p-nuclei the measurements of the integral yields of which have been performed using bremsstrahlung of the Kharkiv electron linear accelerator. The obtained data are compared to the statistical theory of nuclear reactions.

PACS: 26.30.-k, 25.20.-x, 27.60.+j, 29.30.-h, 24.60.Dr

1. INTRODUCTION

Investigations of photonuclear reaction cross sections at the giant resonance region energies made a valuable contribution to understand nuclear interaction and atomic nucleus structure features. In addition, photonuclear reaction data are applied to many technological decisions and penetrated to different sciences promoting their developments. One of the remarkable fields of photonuclear reaction knowledge applications is nuclear astrophysics problems among which the detail understanding of scenarios of origin of chemical elements and their isotopes is crucial to explain the natural abundance.

It is currently established that naturally occurred stable isotopes were mainly resulted from low energy nuclear reactions induced by different particles. Photonuclear reactions play primary role at stellar nucleosynthesis of so called *p-nuclei* ([1] and therein).The last term is used to designate the stable weak abundant isotopes of middle and heavy mass region (between $A = 74$ and $A = 196$) which are located on the proton-rich wing of the isobaric valley of stability but blocked to be produced by the neutron capture s (*slow*)- and/or r (*rapid*)-processes [2, 3], by which the bulk of trans-iron isotopes were synthesized. The scenario in which the p-nuclei are synthesized was primarily named *p-process* that to underline importance of proton capture processes for the production of proton-rich nuclei. However since proton capture reactions required too high temperatures and large densities of stellar medium, photonuclear reactions happening at temperatures $2 \leq T9 \leq 3$ ($T9 = T/10^9 K$) are now considered to have the dominant importance for the p-nuclei production. So the subscenario of the p-nuclei production by complete subsequences of (γ, n), (γ, p) and (γ, α)-reactions was named γ-*process*. The most suitable astrophysical site for the γ-process is the deep oxygen-neon-rich layers of massive stars exploding as type-II supernova [4, 5, 6].

Stellar simulation of the p-nuclei production requires knowledge of the reaction rates of an enormous network of reactions, a large part of which is photodissociation interactions. Moreover, many of these reactions occur on radioactive and excited nuclei of a star interior and therefore cannot be measured under terrestrial conditions. Thereupon theoretical calculations take on special importance. The statistical model of Hauser-Feshbach (H-F) [7] is usually used for this aim since low energy nuclear reactions run through the stage of the compound nucleus formation. Several computer codes [8, 9, 10] implementing the H-F theory are purposely tailored to calculations of the astrophysical reaction cross sections and reaction rates. These codes can by-turn be put to test themselves by comparison with known experimental data.

In recent years some groups performed measurements of photonuclear reaction cross sections on series of middle and heavy nuclei at stellar nucleosynthesis relevant energy region using bremsstrahlung [11, 12, 13, 14, 15] and quasi-monoenergetic photons from Laser Compton Backscattering (see [16, 17, 18] and review [19]) and analyzed them using the H-F model computer codes [8, 9, 10, 20]. However, current databases (cf. KADoNIS database [21]) show the scarce of available data in question. A line of the p-type isotopes are placed in the $A = 90...100$ mass number region. The chains of the molybdenum (Mo), tech-

*Corresponding author E-mail address: semisalovil@kipt.kharkov.ua

netium (Tc), ruthenium (Ru), and rhodium (Rh) isotopes and the ways of their star synthesis are shown in Fig.1. The most of the natural molybdenum (having masses 95 and more) and ruthenium (masses 99 and more) isotopes were synthesized in

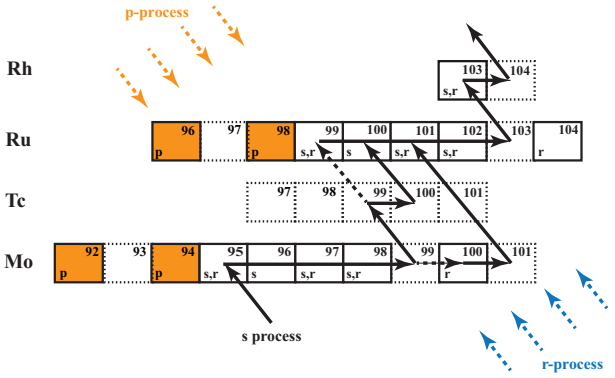

Fig.1. *(Color online) Chains of the molybdenum, technetium, ruthenium, and rhodium isotopes and the main nucleosynthesis processes producing them. The light rectangles with solid and dashed boundaries designate stable s- and/or r-nuclei and radioactive ones, respectively. The orange rectangles designate the 4 p-process nuclei of the molybdenum and ruthenium isotopes*

the s-process (the thick arrow line in Fig.1) and r-process (the individual dashed blue arrows). However both of these scenarios bypass the ^{92}Mo, ^{94}Mo, ^{96}Ru, and ^{98}Ru isotopes (the shaded rectangles). These last naturally occurring isotopes can not be formed by s-process because of the ^{91}Mo, ^{93}Mo, ^{95}Ru, and ^{97}Ru isotope radioactivity and by r-process because of the ^{92}Zr, ^{94}Zr, ^{96}Mo, and ^{98}Mo isotope stability, respectively. A possible chance of these nuclei creation is the p-process (The orange dashed arrows) representing a combination of rapid proton capture reactions (*rp-process*) and (γ, n), (γ, p) or (γ, α) photonuclear reactions (γ-process) on pre-existing s- and r-nuclei as dominant way and the $\nu p - process$ [4] as an alternative one. So if the r-process widens the valley of stability and the s-process elongates it to heavier nuclei then the γ-process moves backward from heavier nuclei to lighter ones.

In the present work we have attempted to adapt the activation technique using bremsstrahlung of the NSC KIPT electron linear accelerator (LINAC) and high resolution gamma-ray spectrometry to study photonuclear reactions in astrophysically relevant energy region. We have measured the integral yields of the (γ, n)-reactions on the ^{96}Ru and ^{98}Ru p-nuclei at the near and above threshold energies and calculated their rates for the nucleus ground states. The $^{197}Au(\gamma, n)^{196}Au$ reaction was used as the standard monitor reaction [22] and the $^{100}Mo(\gamma, n)^{99}Mo$ one [15] to validate the experimental method.

2. FORMULATION OF STELLAR PHOTONUCLEAR REACTIONS

The (γ, n)-reaction rate $\lambda(T)$ for a nucleus disposed in a thermal photon bath of a stellar medium having temperature T is defined by the expression [11]:

$$\lambda(T) = \int_0^\infty c n_\gamma(E_\gamma, T)\, \sigma_{(\gamma,n)}(E_\gamma)\, dE_\gamma\,, \qquad (1)$$

where c is the speed of light, $\sigma_{(\gamma,n)}(E_\gamma)$ the reaction cross section depending on photon energy E_γ and the number of photons $n_\gamma(E_\gamma, T)$ per unit energy and volume of a star interior is noticeably close to the black-body or Planck distribution:

$$n_\gamma(E_\gamma, T) = \left(\frac{1}{\pi}\right)^2 \left(\frac{1}{\hbar\, c}\right)^3 \frac{E_\gamma^2}{\exp(E_\gamma/kT) - 1}\,, \qquad (2)$$

with the Boltzmann constant k.

The Planck distribution is illustrated by the dashed curve (left ordinate axis) in Fig.2 for the stellar plasma temperature $T9 = 3$ which is the relevant temperature of the γ-process.

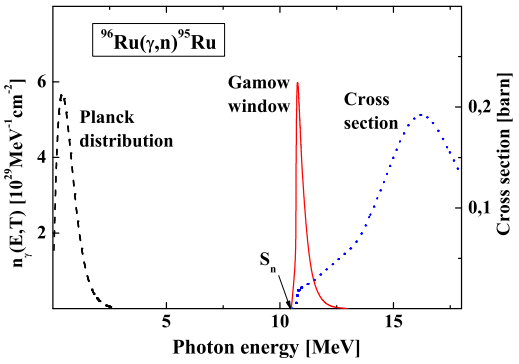

Fig.2. *(Color online) Astrophysically relevant energy range for the (γ, n)-reaction. The dashed black curve (left ordinate axis) is the Planck distribution at $T9 = 3$ temperature, the dotted one (blue in color, right ordinate axis) the excitation function of the $^{96}Ru(\gamma, n)^{95}Ru$ reaction calculated with the NON-SMOKER code [9] of the H-F statistical theory, the solid one (red in color, relative units) the integrand of Eq. 1*

The $^{96}Ru(\gamma, n)^{95}Ru$ reaction excitation function calculated with the NON-SMOKER code [9] of the H-F statistical model is shown by the dotted (blue in color) curve (right ordinate axis). The integrand in Eq. 1 being the product of the steep decreasing and steep increasing functions is represented as a solid curve (red in color) with the sharp maximum at the top energy $E_\gamma = S_n + kT/2$ where S_n is the neutron separation energy, i.e. the (γ, n)-reaction threshold. It is evidently essential at only close and above threshold energy. This peak called the Gamow window by analogy with charged particle induced reactions [23] determines the energy region within of which the (γ, n)-reaction cross sections should be known to derive the reaction rate.

Since there are difficulties concerning radiation strength functions at low energies, the estimated (γ, n)-reaction cross section near threshold can be derived from the Wigner approximation [24]:

$$\sigma_{(\gamma,n)}(E_\gamma) = \sigma_0 \left(\frac{E_\gamma - S_n}{S_n}\right)^{l+1/2}\,, \qquad (3)$$

in which l is the emitted neutron angular momentum ($l = 0$ for s-wave), σ_0 the normalization coefficient which can be learned from the measured activation yield of photonuclear reaction. The cross section $\sigma_{(\gamma,n)}(E_\gamma)$ obtained in such a way can be used to draw the reaction rate.

The scientific group of the Nuclear Physics Institute of the Darmstadt University (Germany) had proposed an alternative method [11, 12] to obtain the photonuclear reaction rate which does not depend on the reaction cross section energy form and consists in approximation of the Planck spectrum by several bremsstrahlung spectra having different end-point energies $E_{0,i}$ at the near and above reaction threshold region (within 1.5...2.0 MeV):

$$cn_\gamma\left(E_\gamma, T\right) \approx \sum_i a_i\left(T\right) \Phi_\gamma\left(E_\gamma, E_{0,i}\right). \qquad (4)$$

Here $a_i(T)$ is a set of the weighting coefficients adjusted for a given stellar environment temperature T, $\Phi_\gamma(E_\gamma, E_{0,i})$ the number of the bremsstrahlung photons per unit energy $[keV]$ and area $[cm^2]$ interval during irradiation. The example for the superposition of the 6 bremsstrahlung spectra calculated by using the Schiff formula [25] for a thin tantalum converter at the end-point energies 10.82, 11.12, 11.30, 11.50, 12.00, and 12.50 MeV (the $^{96}Ru(\gamma,n)^{95}Ru$ reaction threshold equals 10.687 MeV) and multiplied by respective values of the weighting coefficients $a_i(T)$ adjusted for the Planck distribution at temperature $T9 = 3$ is shown in Fig.3. The alternating thin solid and dotted curves imitate the above 6 Schiff bremsstrahlung spectra. The result of their summing is presented by thick solid (red in color) curve. The dashed (blue in color) line is the Planck distribution. The superposition spectrum agrees with the Planck distribution at the high energy bremsstrahlung fairly well. Disagreement below the reaction threshold (the vertical arrow for the $^{96}Ru(\gamma,n)^{95}Ru$ reaction in Fig.3) does not matter.

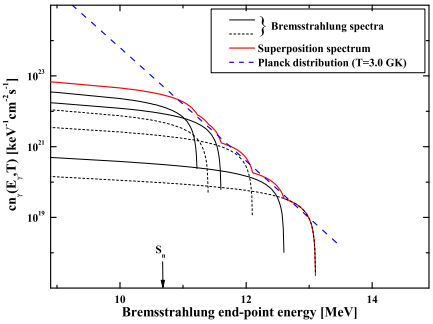

Fig.3. *(Color online) Schiff spectra (alternating thin solid and dotted curves) for the 6 end-point energies (see text), the superposition spectrum (red solid thick curve) for the $^{96}Ru(\gamma,n)^{95}Ru$ reaction and the Planck distribution (blue dashed line) for $T9 = 3$ temperature. The arrow S_n shows the reaction threshold*

Substitution of the thermal Planck spectrum (Eq.4) into Eq.1 gives Eq.5 connecting the reaction rate $\lambda(T)$ and experimental activation yields Y_i measured at the above values of the bremsstrahlung end-point energies:

$$\lambda\left(T\right) = \sum_i a_i\left(T\right) \int_{S_n}^{E_0} \sigma_{(\gamma,n)}\left(E_\gamma\right) \Phi_\gamma\left(E_\gamma, E_{0,i}\right) dE_\gamma \propto \sum_i a_i\left(T\right) Y_i. \qquad (5)$$

So to determine the photonuclear reaction rate by the superposition method one needs to measure the activation integral yields for six or more end-point energies of the bremsstrahlung spectra within the Gamow window range.

3. EXPERIMENTAL

The activation technique with the high resolution γ-spectrometry based on the Ge(Li)-detector was applied for the measurements of the (γ,n)-reaction yields on the ^{96}Ru, ^{98}Ru, and ^{100}Mo nuclei. In contrast to the direct counting of the emitted particle technique, the γ-spectrometry of the specified radioactive residual nuclei makes possible to determine yields of individual reactions using target samples of the natural isotopic composition. Moreover, in many cases simultaneous measurements of yields of reactions occurring on different isotopes of the same chemical element are possible. The latter circumstance is important at the experiments on weak abundant p-nuclei.

3.1. ACCELERATOR OUTPUT AND IRRADIATIONS

The intense bremsstrahlung flux was produced at the Kharkiv LINAC, electron beam energy of which can be varied from 6 to 30 MeV. Fig.4 illustrates the scheme of our experimental setup for irradiation of targets. The electron beam of about 20 μA average operating current was bent on angle of 35° by a sector magnet (not shown in Figure) supplying 3% energy half-width. Having passed through the 50 μm titanium window the beam hit in the 100 μm tantalum converter which was followed by the deflecting magnet to remove any remaining electrons from the photon beam.

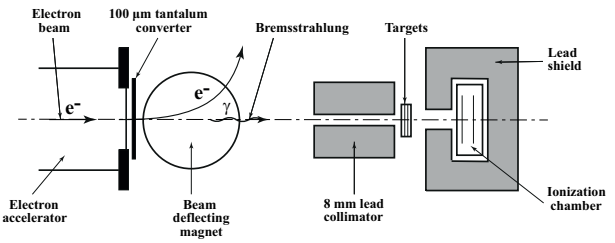

Fig.4. *Sketch of the target irradiation at LINAC*

The stemming Schiff distribution bremsstrahlung was cut by the 8 mm lead collimator of the 100 mm length mounted at the 400 mm distance downstream the converter. Targets of interest elements of natural isotopic composition stacked with the gold foil for the

standard $^{197}Au(\gamma,n)^{196}Au$ reaction were mounted in the container which was positioned on the initial electron beam axis immediately after the collimator.

The ruthenium targets of two types were used at the experiments: (i) available thin (of $\sim 10\,mg/cm^2$ surface density) homogeneous self-supporting foils of the 15 mm diameter made by the electro-deposition technique [26] and (ii) the pressed pills of the high-purity natural ruthenium metallic powder of the $m = (250...300)$ mg and $\oslash = 8$ mm. In the case of the last weight targets, irradiations were carried out with no collimator. The high-purity metallic disks of the 100 μm thickness were used as molybdenum targets while the gold foils of the 20 mm diameter and about 100 mg mass as the standard ones.

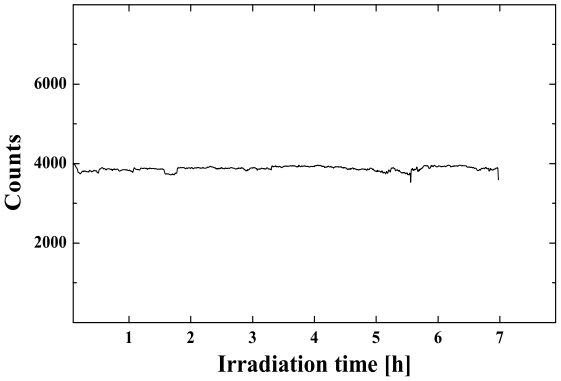

Fig.5. *Typical example of photon flux intensity on a target during 7 hour irradiation monitored by the ionization chamber*

Maximum irradiation time (at low bremsstrahlung end-point energies) reached 7 hours. The photon flux was monitored by regular recording the X-ray dose rate measured by the ionization chamber followed by the target container and screened by the lead shield from side background radiations. Fig.5 shows an example of photon flux intensity as a function of time during irradiation. The necessary corrections were input at the reaction yield calculations in the cases of essential photon flux fluctuations (see below).

3.2. Ge(Li)-DETECTOR

The integral yields of the (γ,n)-reactions under study were determined by the activation equation (see below) from the intensities of the γ-transitions following the β-decays of the produced long-lived radioactive nuclei. γ-Spectra were measured with Ge(Li)-detector located in the low-background room and surrounded with a thick lead shield. The measurements of the absolute detector efficiency having average uncertainty 5% were performed using ^{22}Na, ^{60}Co, ^{133}Ba, ^{137}Cs, ^{226}Ra, and ^{241}Am standard sources. Energy dependences of the detector efficiency for three source-to-detector distance are shown in Fig.6.

The γ-spectrum of each irradiated target was measured many times at different cooling times to identify each peak by the γ-ray energy and half-life of the residual. Distance between source and detector was chosen in this way that the dead time of the acquisition system was not more than 4%. The errors of detector efficiency, statistics, nucleus decay scheme uncertainties and summing effects at high count rate were taken into account at the calculations of the absolute number of the produced nuclei.

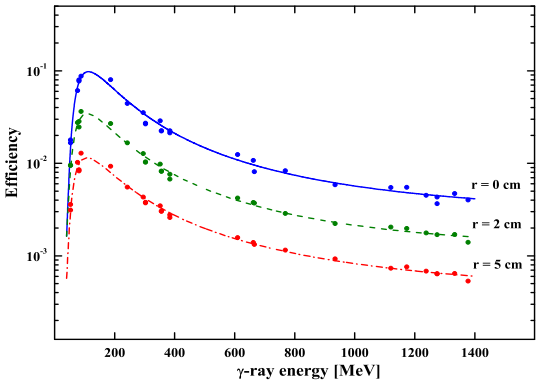

Fig.6. *(Color online) Energy dependence of absolute efficiency of the Ge(Li)-detector for three distances (r) "source-detector"*

3.3. DECAY FEATURES OF THE RESIDUAL RADIOISOTOPES AND ACTIVITY MEASUREMENTS

The decay schemes of the radioactive nuclei ^{95}Ru and ^{97}Ru produced in the studied $^{96}Ru(\gamma,n)^{95}Ru$ and $^{98}Ru(\gamma,n)^{97}Ru$ reactions as well as ^{196}Au and ^{99}Mo as the products of the standard $^{197}Au(\gamma,n)^{196}Au$ and test $^{100}Mo(\gamma,n)^{99}Mo$ reactions are presented in Fig.7.

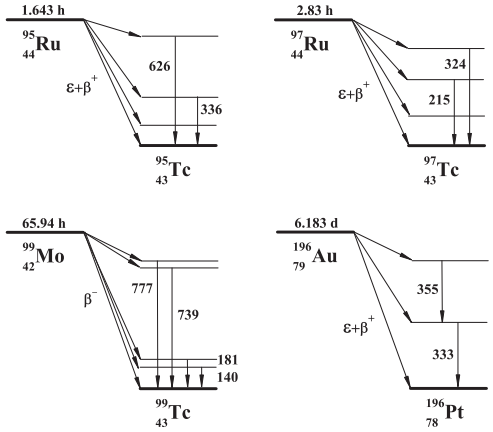

Fig.7. *Simplified decay schemes of the ^{95}Ru, ^{97}Ru, ^{99}Mo and ^{196}Au residual radionuclides*

Numerical data of the reaction thresholds, half-lives, energies, and branching ratios of the observed γ-transitions are given in Table. Fig.8 presents the examples of the γ-ray spectra emitted by the Ru (upper panel), Mo (middle panel), and Au (lower panel) targets irradiated by the 13 MeV end-point energy bremsstrahlung.

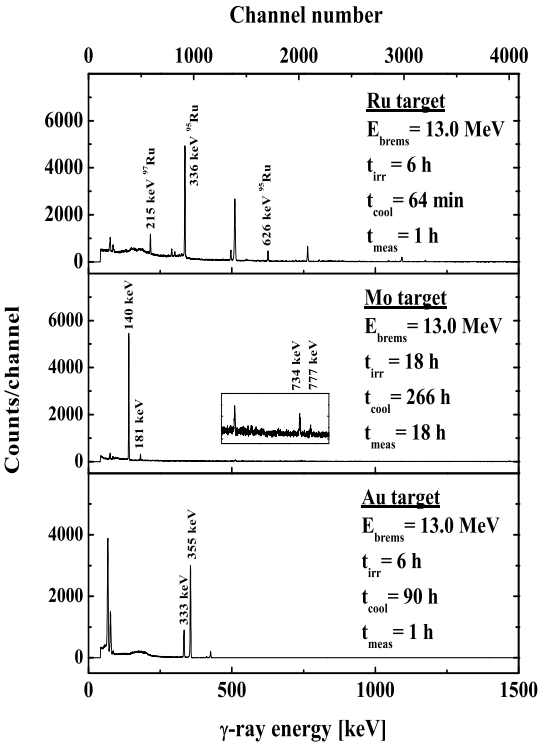

Fig.8. *Decay $\gamma-$ray spectra of the ruthenium (upper panel), molybdenum (middle panel) and gold (lower panel) targets irradiated with the 13 MeV end-point energy bremsstrahlung*

The times of irradiation (t_{irr}), cooling (t_{cool}) and measurement (t_{meas}) are shown in the panels. Each peak of these spectra corresponds to full energy absorption of corresponding γ-rays following the decay of one or another long-lived radioactive nucleus. Reaction activation yields can be calculated from the intensities of these peaks: for ^{95}Ru formation via the intensities of the γ-ray lines 336 and 626 keV, ^{97}Ru 215 and 324 keV, ^{99}Mo 140, 181, 739, and 777 keV and ^{196}Au 333 and 355 keV (see Table).

3.4. ACTIVATION YIELD CALCULATIONS

The experimental integral yield $Y_{act}(E_0)$ of a (γ, n)-reaction normalized to one target nucleus and unit bremsstrahlung flux of end-point energy E_0 is determined from the intensity N_γ of the corresponding γ-line via the conventional activation equation:

$$Y_{act}\,(E_0) = \frac{N_\gamma}{N_{targ}\lambda t_{irr}\varepsilon B}\exp(\lambda t_{cool}) \times \\ \times\{[1-\exp(-\lambda t_{irr})][1-\exp(-\lambda t_{meas})]\}^{-1}, \quad (6)$$

in which N_{targ} is the number of the target nuclei, λ the radioactive decay constant, ε the detector efficiency, B the branching ratio of the observed γ-transition, t_{irr}, t_{cool} and t_{meas} the times of irradiation, cooling and measurement of the sample activity, respectively. Eq.6 is correct in the case of constant bremsstrahlung flux. If there are its remarkable fluctuations during irradiation time we used the activation equation in the form:

$$Y_{act}\,(E_0) = \frac{N_\gamma}{N_{targ}\lambda t_{irr}\varepsilon B}\{[1-\exp(-\lambda t_{meas})] \times \\ \times\sum_{j=1}^{n}\frac{I_j}{I_{total]}}[1-\exp(-\lambda\Delta t^j_{irr})]\exp(-\lambda\Delta t^j_{cool})\}^{-1}, \quad (7)$$

where $\frac{I_j}{I_{total}}$ is the ratio of number of counts of the ionization chamber in j-th irradiation interval to the total number of counts during n intervals, Δt^j_{irr} and Δt^j_{cool} the lengths of j-th irradiation interval and corresponding cooling time, respectively.

Reaction thresholds and used spectroscopic data of residual nuclei [27]

Reaction	Reaction threshold [MeV]	Residual nucleus	Half life	Eg [keV]	Branching ratio [%]
$^{96}Ru(g,n)$	10.693	^{95}Ru	1.643 h	336.4	70.1 (5)
				626.8	17.8(5)
$^{98}Ru(g,n)$	10.189	^{97}Ru	2.83 d	215.7	86 (5)
				324.5	10.8(2)
$^{100}Mo(g,n)$	8.289	^{99}Mo	65.976 h	140.5	89(3)
				181.1	5.99(7)
				739.5	12.26(18)
				777.9	4.3(8)
$^{197}Au(g,n)$	8.071	^{196}Au	6.1669 d	333.0	22.9(9)
				355.7	87(3)

On the other hand (γ, n)-reaction yield is a convolution of the cross section $\sigma_{(\gamma,n)}(E_\gamma)$ with the bremsstrahlung absolute spectrum $\Phi_\gamma(E_\gamma, E_0)$ over the photon energies:

$$Y_{act}\,(E_0) = \int_{S_n}^{E_0} \sigma_{\gamma,n}\,(E_\gamma)\,\Phi_\gamma\,(E_\gamma, E_0)\,dE_\gamma. \qquad (8)$$

As it was noticed in section 3.1 the reaction $^{197}Au(\gamma, n)^{196}Au$ was used as the standard one for determination of the bremsstrahlung fluence. Apart from earlier works the thorough researches of this reaction have been revived after the year 2000 in conjunction with the study of the γ-process stellar nucleosynthesis. A number of scientific teams have measured and analyzed its cross sections using bremsstrahlung [22, 28, 29, 30] and laser Compton scattering γ-rays [31, 32, 33] paying attention to the low energy region. Fig.9 illustrates the experimental values (points) of the $^{197}Au(\gamma, n)^{196}Au$ reaction cross sections obtained in three recent works [31, 32, 33] which are in accordance each with other, and the fitted curve for the last data set ranging to the near threshold energy region.

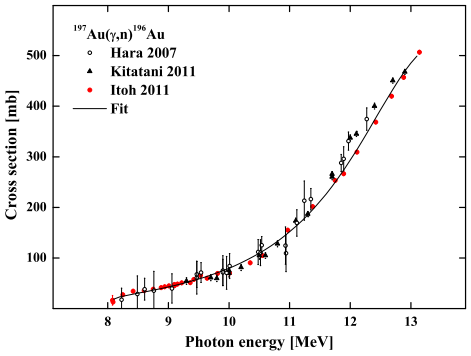

Fig.9. *(Color online) Excitation function of the $^{197}Au(\gamma, n)^{196}Au$ reaction measured by different teams. The points denote the experimental data of Hara et al. [31], Kitatani et al. [32] and Itoh et al. [33] the curve is polynomial fitting of Itoh et al. data (red points)*

The experimental integral yield values of the studied and standard reactions derived from the activities of the targets of the same irradiation together with absolute cross sections of the $^{197}Au(\gamma, n)^{196}Au$ reaction (the fitted curve in Fig.9) give possibility to draw the rates of the studied reactions. In practice we used the activation yield of the studied reaction reduced to the gold reaction one, i.e.

$$Y_{act}^{red} = \frac{Y_{act}(Target)}{Y_{act}(Au)}. \qquad (9)$$

4. THE EXPERIMENTAL RESULTS AND COMPARISON WITH THE THEORETICAL PREDICTIONS

We set ourselves as an object (i) to determine the activation yields of the (γ, n)-reactions running on the p-nuclei ^{96}Ru and ^{98}Ru in order (ii) to derive the reaction rates at astrophysically interesting energy region and (iii) to compare them with the theoretical predictions.

4.1. REACTION YIELDS

The experimental integral yields of the reactions $^{96}Ru(\gamma, n)^{95}Ru$, $^{98}Ru(\gamma, n)^{97}Ru$ as well as $^{100}Mo(\gamma, n)^{99}Mo$ as the test reaction calculated with the activation equation are shown in Fig.10 as the function of the bremsstrahlung end-point energy.

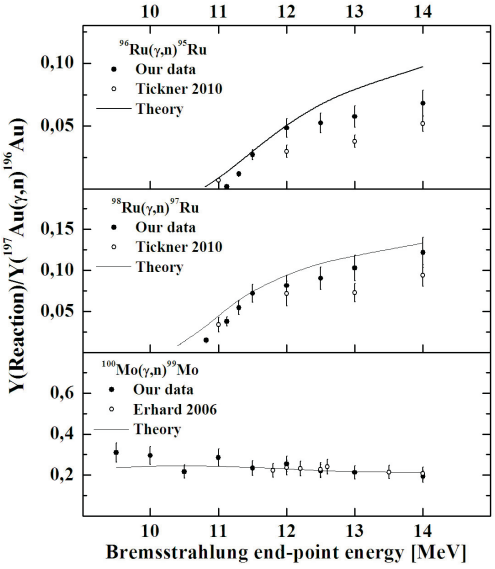

Fig.10. *Experimental (points) and theoretical (curves) integral yields of the (γ, n)-reactions on ^{96}Ru, ^{98}Ru and ^{100}Mo reduced to the standard $^{197}Au(\gamma, n)^{196}Au$ reaction integral yields depending on the bremsstrahlung end-point energy*

The data are normalized to the standard $^{197}Au(\gamma, n)^{196}Au$ reaction yields. The dark points represent our results while the light ones depict the Tickner et al. data [34] for the two first reactions and the Erhard et al. data [15] for the last one. The agreement between results of ours and aforementioned authors can be considered as satisfactory. The solid curves in graphs represent the theoretical values calculated in the frame of the H-F statistical model incorporated by the NON-SMOKER code [9] with the default input parameters providing a global description for a wide range of isotopes: the neutron optical potential of Jeukenne et al. [35] with a low-energy modification of Lejeune [36], the radiation strength function of Thielemann and Arnold [37] and nuclear level density of the back-shifted Fermi-gas model formalized by Rauscher et al. [38].

4.2. REACTION RATES

Fig.11 illustrates the experimental and theoretical values of the reaction rates (vertical logarithmic axis)

in the most significant range of temperatures (horizontal axis) for the γ-process stellar nucleosynthesis located between $T9 = 2$ and $T9 = 3$.

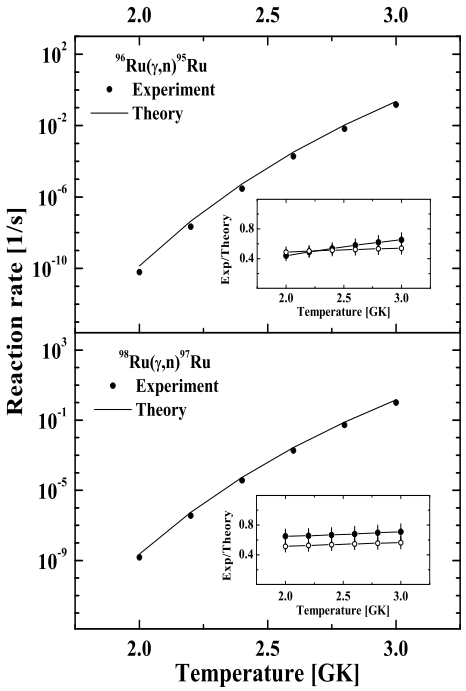

Fig.11. *Experimental (points) and theoretical (NON-SMOKER code) reaction rates of the $^{96}Ru(\gamma,n)^{95}Ru$ (upper panel) and $^{98}Ru(\gamma,n)^{97}Ru$ (lower panel) reactions on dependence of star environment temperatures inherent to the $\gamma-process$ nucleosynthesis. Inserts are the ratios (linear ordinate) of experimental values calculated using Wigner approximation for the cross section energy dependence (dark points) and superposition technique (light points) to the theory predictions*

The upper and lower graphs show the results for the $^{96}Ru(\gamma,n)^{95}Ru$ and $^{98}Ru(\gamma,n)^{97}Ru$ reactions, respectively. The points depict the reaction rates calculated from the measured activation integral yields while the curves from the theoretical values of the cross sections predicted by the H-F statistical model code NON-SMOKER [9]. As seen in the main plots of Fig.11 the agreement of the experimental and theoretical reaction rates of each reaction is fairly well in general despite the large difference between the absolute values for the two studied reactions that is caused by the different threshold energies (see Table). More detailed visualization is presented in the inserts of the panels where the ratios of the experimental reaction rate values calculated with the Wigner approximation (dark points) and superposition technique (light points) to the theoretical predictions are shown. Both approximations give the similar results but the theoretical predictions overestimate the reaction rates by (40...60)% in the considered temperature range.

5. CONCLUSIONS

The activation technique using the bremsstrahlung of the NSC KIPT LINAC and gamma-ray spectrometry was put to the test for the measurements of the integral yields of the reactions $^{96}Ru(\gamma,n)^{95}Ru$ and $^{98}Ru(\gamma,n)^{97}Ru$ in order to determine the reaction rates in the astrophysically interesting energy region just above the neutron emission threshold. The default option of the NON-SMOKER code of the statistical theory of nuclear reactions overestimates the experimental reaction rates within a factor of about 2. Similar measurements at NSC KIPT can be extended in the nuclear mass number region $A \sim 100$ containing a number of p-nuclei to supplement the network of astrophysical photonuclear reactions for the γ-process stellar nucleosynthesis simulation and to test the statistical model parametrization.

ACKNOWLEDGEMENTS

The authors express their gratitude to Dr. S. Gokov and the LINAC staff for providing target irradiation procedure.

References

1. T. Rauscher. Origin of the p-nuclei in explosive nucleosynthesis // *Nuclei in the Cosmos XI, Heidelberg, Ed. by K. Blaum, N. Christlieb, G. Martinez-Pinedo, 2010, Proceedings of Science*, PoS(NIC XI) 059.
2. E.M. Burbidge, G.R. Burbidge, W.A. Fowler and F. Hoyle. Synthesis of the elements in stars // *Rev. Mod. Phys.* 1957, v. 29, p. 547-650.
3. A.G.W. Cameron. Nuclear reactions in stars and nucleogenesis // *Publications of the Astronomical Society of the Pacific.* 1957, v. 69, p. 201-222.
4. M. Arnold, S. Goriely. The p-process of stellar nucleosynthesis: astrophysics and nuclear physics status // *Phys. Rep.* 2003, v. 384, p. 1-84.
5. W. Rapp, J. Gorres, M. Wiescher, H. Schatz, F. Kappeler. Sensitivity of p-process nucleosynthesis to nuclear reaction rates in a 25 $M_\circ$ supernova model // *Astrophys. J.* 2006, v. 653, p. 474-489.
6. T. Rauscher. Branchings in the γ-process path revisited // *Phys.Rev.* 2006, v. C73, p. 015804.
7. W. Hauser and H. Feshbach. The inelastic scattering of neutrons // *Phys. Rev.* 1952, v. 87, p. 366-373.
8. T. Rauscher, F.-K. Thielemann. Astrophysical reaction rates from statistical model calculations // *At. Data Nucl. Data Tables.* 2000, v. 75, p. 1-351.

9. T. Rauscher, F.-K. Thielemann. Predicted cross-sections for photon-induced particle emission // *At. Data Nucl. Data Tables.* 2004, v. 88, p. 1-81.

10. S. Goriely. Hauser-Feshbach reaction rates for nuclei with $Z = 8...109$ // *Proc. of Capture Gamma-Ray Spectroscopy and Related Topics / Ed. by S. Wender. - AIP Conf. Proc.* N529 Melville, NY, 2000, p. 287; see also http://www-astro.ulb.ac.be.

11. P. Mohr, K. Vogt, M. Babilon, J. Enders, T. Hartmann, C. Hutter, T. Rauscher, S. Volz, A. Zilges. Experimental simulation of a stellar photon bath by bremsstrahlung: the astrophysical γ-process // *Phys. Lett.* 2000, v. B488, p. 127-130.

12. K. Vogt, P. Mohr, M. Babilon, J. Enders, T. Hartmann, C. Hutter, T. Rauscher, S. Volz, A. Zilges. Measurement of the (γ, n) reaction rates of the nuclides ^{190}Pt, ^{192}Pt, and ^{198}Pt in the astrophysical γ-process // *Phys. Rev.* 2001, v. C63, p. 055802.

13. K. Sonnabend, K. Vogt, D. Galaviz, S. Muller, A. Zilges. Systematic study of (γ, n) reaction rates for $Z \geq 78$ isotopes // *Phys. Rev.* 2004, v. C70, p. 035802.

14. J. Hasper, D. Galaviz, S. Muller, A. Sauerwein, D. Savran, L. Schnorrenberger, K. Sonnabend, A. Zilges. Investigation of photoneutron reactions on ^{192}Os and ^{191}, ^{193}Ir at energies of relevance for the astrophysical p-process // *Phys. Rev.* 2009, v. C79, p. 055807.

15. M. Erhard, A.R. Junghans, R. Beyer, E. Grosse, J. Klug, K. Kosev, C. Nair, N. Nankov, G. Rusev, K.D. Schilling, R. Schwengner, and A. Wagner. Photodissociation of p-process nuclei studied by bremsstrahlung-induced activation // *Eur. Phys. J.* 2006, v. A27, Supp. 1, p. 136-140.

16. H. Utsunomiya, A. Makinaga, S. Goko, T. Kaihori, H. Akimune, T. Yamagata, M. Ohta, H. Toyokawa, S. Muller, Y.-W. Lui, S. Goriely. Photoneutron cross section measurements on the $N = 82$ nuclei ^{139}La and ^{141}Pr: Implications for p-process nucleosynthesis // *Phys.Rev.* 2006, v. C74, p. 025806

17. H. Utsunomiya, S. Goko, H. Toyokawa, H. Ohgaki, K. Soutome, H. Yonehara, S. Goriely, P. Mohr, Zs. Fulop. Photonuclear reaction data and γ-ray sources for astrophysics // *Eur. Phys. J.* 2006, v. A27, Supp.1, p. 153-158.

18. K. Sonnabend, J. Hasper, S. Muller, N. Pietralla, D. Savran, L. Schnorrenberger, A. Zilges. Activation experiments for nuclear astrophysics // *Proc.13th Intern.Symposium on Capture Gamma-Ray Spectroscopy and Related Topics, Cologne, Germany*, 25-29 Aug.2008. J. Jolie, A. Zilges, N. Warr, A. Blazhev, Eds., 2009, p. 481-485; AIP Conf.Proc. 1090, 2009.

19. H. Utsunomiya, P. Mohr, A. Zilges, M. Rayet. Direct determination of photodisintegration cross sections and the p-process // *Nucl.Phys.* 2006, v. A777, p. 459-478.

20. A.J. Koning, S. Hilaire, M.C. Duijvestijn. TALYS: Comprehensive nuclear reaction modeling // *Proc. Intern. Conf. Nuclear Data for Science and Technology, Santa Fe, New Mexico, USA*, 26 September-1 October, 2004. R.C. Haight, M.B. Chadwick, T. Kawano, P. Talou, Eds., 2005, v. 2, p. 1154-1159; AIP Conf. Proc. 769, 2005.

21. http://nuclear-astrophysics.fzk.de/kadonis/

22. K. Vogt, P. Mohr, M. Babilon, W. Bayer, D. Galaviz, T. Hartmann, C. Hutter, T. Rauscher, K. Sonnabend, S. Volz, A. Zilges. Measurement of the (γ, n) cross section of the nucleus ^{197}Au close above the reaction threshold // *Nucl.Phys.* 2002, v. A707, p. 241-252.

23. C. Rolfs, H.P. Trautvetter, W.S. Rodney. Current status of nuclear astrophysics // *Rep. Prog. Phys.* 1987, v. 50, p. 233-325.

24. E.P. Wigner. On the behavior of cross sections near thresholds // *Phys. Rev.* 1948, v. 73, p. 1002-1009.

25. L.I. Schiff. Energy-angle distribution of thin target bremsstrahlung // *Phys. Rev.* 1951, v. 83, p. 252-253.

26. A.P. Kljucharev, L.I. Kovalenko, L.G. Lishenko, V.N. Medjanik, T.S. Nazarova, A.A. Rozen. *Thin Foils of Metal Isotopes. Preparation Methods.*, Moscow: "Energoizdat", 1981, p. 62-81.

27. http://www.nndc.bnl.gov/nudat2/

28. C. Nair, M. Erhard, A.R. Junghans, D. Bemmerer, R. Beyer, E. Grosse, J. Klug, K. Kosev, G. Rusev, K.D. Schilling, R. Schwengner, A. Wagner. Photoactivation experiment on ^{197}Au and its implications for the dipole strength in heavy nuclei // *Phys.Rev.* 2008, v. C78, p. 055802.

29. C. Plaisir, F. Hannachi, F. Gobet, M. Tarisien, M. M. Aleonard, V. Meot, G. Gosselin, P. Morel, B. Morillon. Measurements of the $^{85}Rb(\gamma, n)^{84m}Rb$ cross section in the energy range 10...19 MeV with bremsstrahlung photons // *Eur. Phys. J.* 2012, v. 48, p. 68-72.

30. V.V. Varlamov, B.S. Ishkhanov, V.N. Orlin, S.YU. Troschiev. New data for $^{197}Au(\gamma, nx)$ and $^{197}Au(\gamma, 2nx)$ reaction cross sections // *Izv. Rossiiskoi Akademii Nauk. Ser. "Fiz."* 2010, v. 74, p. 884-891.

31. K.Y. Hara, H. Harada, F. Kitatani, S. Goko, S. Hohara, T. Kaihori, A. Makinaga, H. Utsunomiya, H. Toyokawa, K. Yamada. Measurements of the $^{152}Sm(\gamma, n)$ cross section with laser-compton scattering γ rays and the photon difference method // *Jour. of Nuclear Science and Technology.* 2007, v. 44, p. 938-945.

32. F. Kitatani, H. Harada, S. Goko, H. Utsunomiya, H. Akimune, H. Toyokawa, and K. Yamada. Measurement of ^{76}Se and $^{78}Se(\gamma, n)$ cross sections // *Jour. of Nuclear Science and Technology.* 2011, v. 48, p. 1017-1024.

33. O. Itoh, H. Utsunomiya, H. Akimune, T. Kondo, M. Kamata, T. Yamagata, H. Toyokawa, H. Harada, F. Kitatani, S. Goko, C. Nair, Y.-W. Lui. Photoneutron cross sections for Au revisited: measurements with laser Compton scattering γ-rays and data reduction by a least-squares method // *Jour. of Nuclear Science and Technology.* 2011, v. 48, p. 834-840.

34. J. Tickner, R. Bencardino, G. Roach. Measurement of activation yields for platinum group elements using Bremsstrahlung radiation with endpoint energies in the range 11...14 MeV // *Nucl. Instr. and Meth.in Phys. Res.* 2010, B268, p.99-105.

35. J.-P. Jeukenne, A. Lejeune, and C. Mahaux. Optical-model potential in finite nuclei from reid's hard core interaction // *Phys. Rev.* 1977, v. C16, p. 80-96.

36. A. Lejeune. Low-energy optical potential in finite nuclei from Reid's hard core interaction // *Phys. Rev.* 1980, v. C21, p. 1107-1108.

37. F.-K. Thielemann and M. Arnold. In Praceedings of the International Conference on Nuclear Data for Science and Technology, editted by K. Beckhoff (Reidel, Dorgreht, 1983), p.762.

38. T. Rauscher, F.-K. Thielemann, K.-L. Kratz. Nuclear level density and the determination of thermonuclear rates for astrophysics // *Phys. Rev.* 1997, v. C56, p. 1613-1625.

АКТИВАЦИОННАЯ МЕТОДИКА ИЗМЕРЕНИЯ СКОРОСТЕЙ АСТРОФИЗИЧЕСКИХ ФОТОЯДЕРНЫХ РЕАКЦИЙ НА ПУЧКЕ ТОРМОЗНОГО ИЗЛУЧЕНИЯ

И. Семисалов, Е. Скакун, В. Касилов, В. Попов

Астрофизическое моделирование природной распространённости так называемых p-изотопов требует сведений о скоростях низкоэнергетичных (припороговых) фотоядерных реакций на огромном числе атомных ядер. На примере (γ, n)-реакций, вызываемых фотонами в ядрах p-изотопов ^{96}Ru и ^{98}Ru, продемонстрирована возможность получения соответствующей экспериментальной информации на пучке тормозного излучения харьковского линейного ускорителя электронов путём измерения интегральных выходов реакций. Полученные результаты сравниваются с предсказаниями статистической теории ядерных реакций.

АКТИВАЦІЙНА МЕТОДИКА ВИМІРЮВАННЯ ШВИДКОСТЕЙ АСТРОФІЗИЧНИХ ФОТОЯДЕРНИХ РЕАКЦІЙ, НА ПУЧКУ ГАЛЬМІВНОГО ВИПРОМІНЮВАННЯ

І. Семісалов, Є. Скакун, В. Касілов, В. Попов

Астрофізичне моделювання природної розповсюдженості так званих p-ізотопів потребує знань швидкостей низькоенергетичних (припорогових) фотоядерних реакцій на величезній кількості атомних ядер. На прикладі (γ, n)-реакцій, спричиняємих гальмівним випромінюванням харківського лінійного прискорювача електронів в ядрах p-ізотопів ^{96}Ru та ^{98}Ru, продемонстровано можливість отримання відповідної експериментальної інформації шляхом вимірювання інтегральних виходів реакцій. Отримані результати порівнюються з передбаченнями статистичної теорії ядерних реакцій.